



Taverne, M. P. C., Zeng, X., Morgan, K. A., Zeimpekis, I., Huang, C. C., Ho, Y. L. D., Mostafavi, M., & Shterenlikht, A. (2018). Fabrication of micro-scale fracture specimens for nuclear applications by direct laser writing. *MRS Advances*, 3(31 (Energy and Sustainability)), 1771-1775. <https://doi.org/10.1557/adv.2018.236>

Peer reviewed version

Link to published version (if available):
[10.1557/adv.2018.236](https://doi.org/10.1557/adv.2018.236)

[Link to publication record in Explore Bristol Research](#)
PDF-document

This is the author accepted manuscript (AAM). The final published version (version of record) is available online via Cambridge University Press at <https://www.cambridge.org/core/journals/mrs-advances/article/fabrication-of-microscale-fracture-specimens-for-nuclear-applications-by-direct-laser-writing/2D49C6C6046FD6670ABEFB2E19DD48DC> . Please refer to any applicable terms of use of the publisher.

University of Bristol - Explore Bristol Research

General rights

This document is made available in accordance with publisher policies. Please cite only the published version using the reference above. Full terms of use are available:
<http://www.bristol.ac.uk/red/research-policy/pure/user-guides/ebr-terms/>

Fabrication of micro-scale fracture specimens for nuclear applications by direct laser writing

Mike P.C. Taverne^{1,2}, Xu Zeng^{1,2}, Katrina A. Morgan³, Ioannis Zeimpekis³, Chung-Che Huang³, Ying-Lung D. Ho², Mahmoud Mostafavi¹, Anton Shterenlikht^{1,*}

¹ Department of Mechanical Engineering, University of Bristol, Bristol, BS8 1TR, UK

² Department of Electrical and Electronic Engineering, University of Bristol, Bristol BS8 1UB, UK

³ Optoelectronics Research Centre, University of Southampton, Southampton SO17 1BJ, UK

* E-mail: mexas@bristol.ac.uk

ABSTRACT

The structural integrity of nuclear fission and fusion power plant components is the focus of this research. The state of the art is using micro scale specimens milled with a focussed ion beam (FIB). Because of their very low volume such specimens can be lab tested, even when irradiated to low or medium level of activity. This offers a possibility of testing multiple specimens to investigate stochastic effects, e.g. effects of irradiation on the shift of the ductile to brittle transition. However, FIB milled specimens suffer from Ga contamination, to the degree that the validity of fracture data obtained on such specimens is questionable. We propose to use nano-additive manufacturing as an alternative to FIB for making micro scale fracture specimens. A combination of two-photon polymerization and electrodeposition and sputtering was used to manufacture micro-scale Brazilian disk fracture specimens (CBD), which are free from Ga and thus better suited for the study of irradiation effects on structural integrity. In this study Ni CBD specimens were made with 30 μm diameter and up to 13 μm thickness. The slot width varied between 1 μm to 2.9 μm with the corresponding slot length of between 7.5 μm and 8 μm . Consecutive FIB characterization shows that the specimens have polycrystalline microstructure with sub- μm grains. The work is ongoing making W CBD specimens and on reducing the slot width and using chemical vapor deposition fabrication.

INTRODUCTION

Recently, considerable efforts have been dedicated to micromechanical testing of small scale specimens whose microstructure can be characterized by various advanced techniques such as scanning electron microscopy [1], high resolution transmission electron microscopy [2], atom probe tomography [3], and X-ray nano-tomography [4]. This is because such small-scale tests can be ion implanted or neutron irradiated but still handled in laboratory conditions due to their small volume even if the samples show low to medium levels of activity. The currently accepted method for fabricating micro-specimens is micro-milling micro-pillars or micro-cantilever beams, which undergo compression or bend loading by using a nano-indenter. The milling is carried out by focused ion beams (FIB). The process, although extremely versatile, is known to induce damage and material alterations to the specimens; these include: Ga contamination [5], Ga segregation to grain boundaries [6], change in the stoichiometry [7], and in extreme cases amorphization [8]. Helium FIB suffers from similar issues (e.g. helium bubbles implantation). In addition to inducing damage, FIB milling limits the geometry of fabricated specimens. For example, the notched micro cantilever beams used in measuring fracture toughness do not allow for accurate measurement of the crack morphology, length, and interaction with the microstructure [9]. FIB cannot be used to mill very deep narrow slits, because material atoms displaced by impacts with Ga ions cannot escape from deep narrow slits. This results in the fracture toughness extracted from micro-samples to be unreliable.

In this work we explore the feasibility of using additive manufacturing techniques as alternatives to FIB milling. We show that direct laser writing by two-photon polymerization (2PP-DLW) is a highly accurate and flexible technique, that can be used for creating complex 3D geometries (templates). We then show how such templates can be used to make micro-specimens via different materials deposition methods [10].

GEOMETRIC DESIGN

The specimen geometry is a cracked Brazilian disk (CBD), as illustrated in Fig. 1a. It is a disk, with a thin slot along one axis. Blocks are added on the top and bottom of the disk so that pressure can be applied more easily along the length of the slot for fracture testing. The design parameters are detailed in Fig. 1b. The original design was $D = 15 \mu\text{m}$, $W = 1 \mu\text{m}$, $L = 5 \mu\text{m}$ and $B = 2 \mu\text{m}$. However, due to initial fabrication issues, such as size variation after material

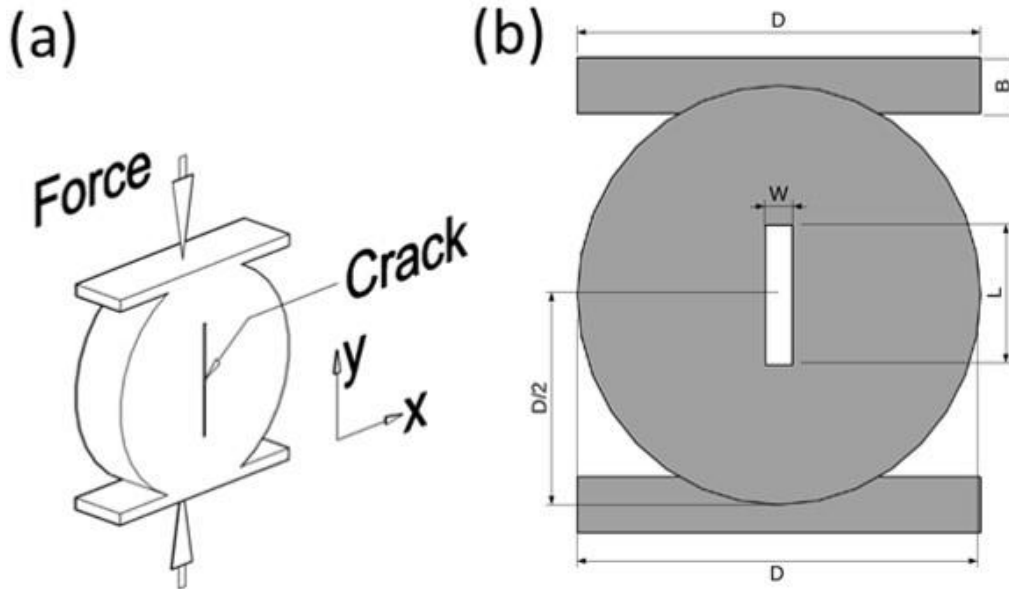


Figure 1. (a) Cracked Brazilian Disk (CBD) – the crack opens in x direction due to Poisson effect when compressive force is exerted on the sample in y direction. The crack is expected to grow in the y direction. (b) CBD design parameters.

deposition, all dimensions were doubled in order to first establish the feasibility of backfilling via electrodeposition. Hence, the parameters used in this paper are: $D = 30 \mu\text{m}$, $W = 2 \mu\text{m}$, $L = 10 \mu\text{m}$ and $B = 4 \mu\text{m}$. Additionally, the nominal slot width W was varied from 2 to $8 \mu\text{m}$ in $2 \mu\text{m}$ steps (2, 4, 6, $8 \mu\text{m}$).

SPECIMEN PREPARATION AND FABRICATION

In this paper, a micro-scale fracture specimen was fabricated by 2PP-DLW [11-12], followed by Ni electrodeposition. Fig. 2 illustrates the manufacturing processes for producing specimens. There are four steps for creating a CBD specimen. First, a positive resist (AZ9260) was spun onto an ITO-coated coverslip glass substrate yielding a thickness of approximately $13 \mu\text{m}$. Then, a two-photon lithography system (consisting of a laser wavelength 780 nm , power 120 mW laser with pulse width 120 fs and rep rate 80 MHz) was used to write structures within the resist. Following this, polymeric templates (an inverse CBD, as shown in Fig. 3) were made, where the laser power was varied between $4\text{-}10 \text{ mW}$ and development time was about 8.5 minutes ($40 \text{ s}/\mu\text{m}$). The next step was electrodeposition. In this process, Ni was used to backfill the templates. A standard Watts bath (700 ml) was used consisting of Ni sulphate (168 g), Ni chloride (22 g), and boric acid (21 g). A simple two-electrode implementation was used with a Ni anode and operating at constant current of 2 mA . After electrodeposition, the resist was lifted off for 10 minutes in acetone. Fig. 3 shows step 2 of the process: the polymer template (or mold) obtained after developing the positive photoresist after writing the CBDs into it. The exposed areas are removed, leaving a hollow disk shape, with a wall for the disk slot.

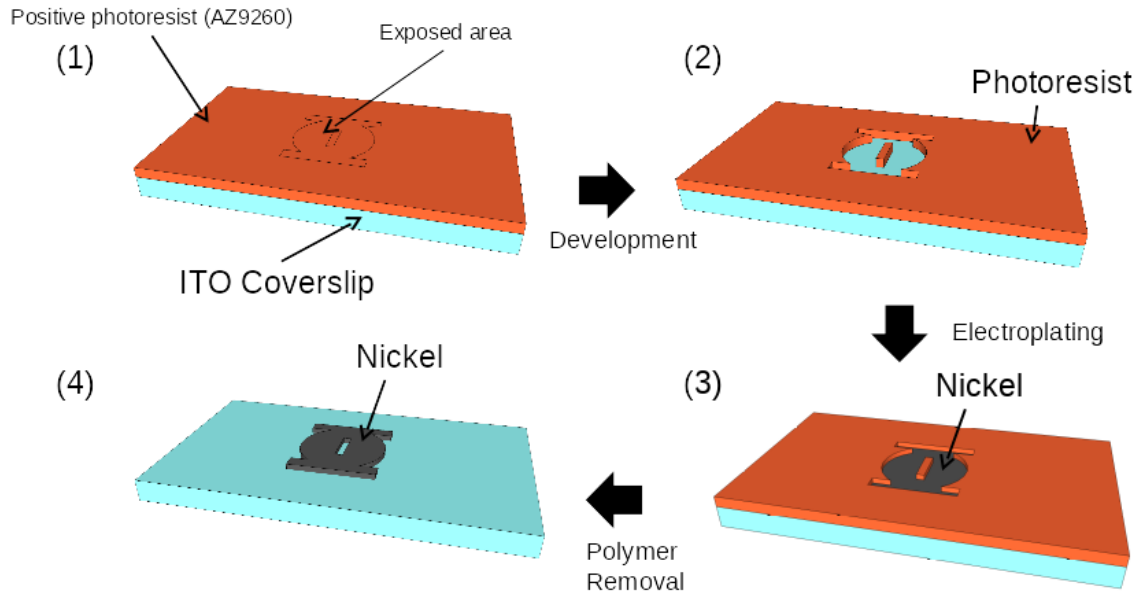


Figure 2. Schematic illustrating the CBD fabrication process with direct laser writing and electrodeposition. The four steps of fabrication: (1) Direct laser writing, (2) development, (3) Electroplating, (4) Polymer removal in acetone.

RESULTS AND DISCUSSION

FIB images of the Ni CBD specimens are shown in Fig. 4. The nominal slot size was $2 \times 10 \mu\text{m}^2$ and the specimen had a maximum height of $8.7 \mu\text{m}$. The specimen shows clearly visible layers, which are about $3 \mu\text{m}$ thick. This is due to the slicing distance between layers being too large in the input file used during the DLW process. This problem can be eliminated by reducing the layer thickness and increasing the number of layers. Fig. 4(b-e) shows cross-sections of the specimen, made with a FIB, along the X direction (b-c) and along the Y direction (d-e). The inside of the disk looks heterogeneous. This could be due to impurities in the electrodeposition solution or other electrodeposition related issues (irregular or too high/low currents for example).

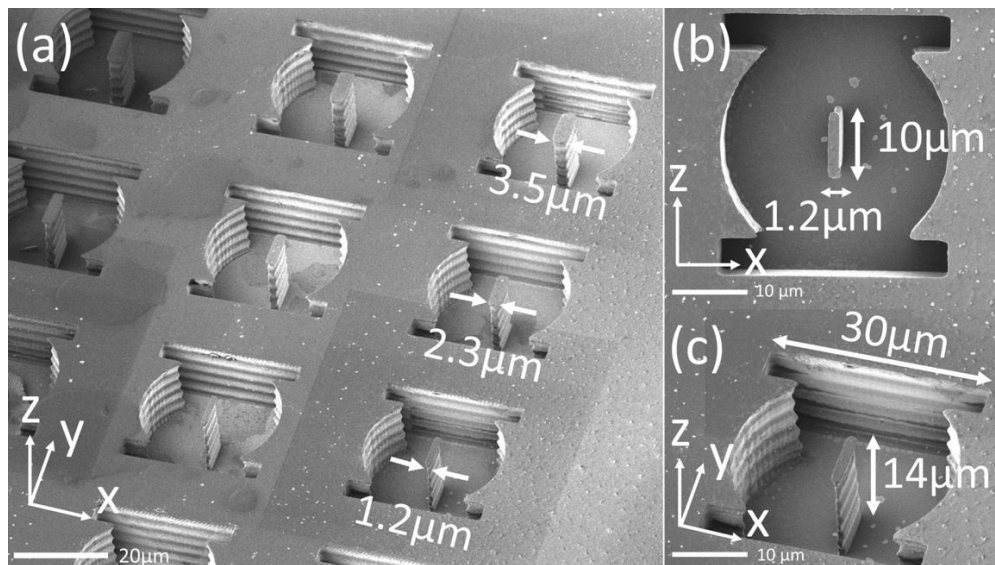


Figure 3. SEM images (a) an array of polymeric CBD templates fabricated by two-photon polymerization lithography. (b) zoom in of top view and (c) 45° view of a single CBD.

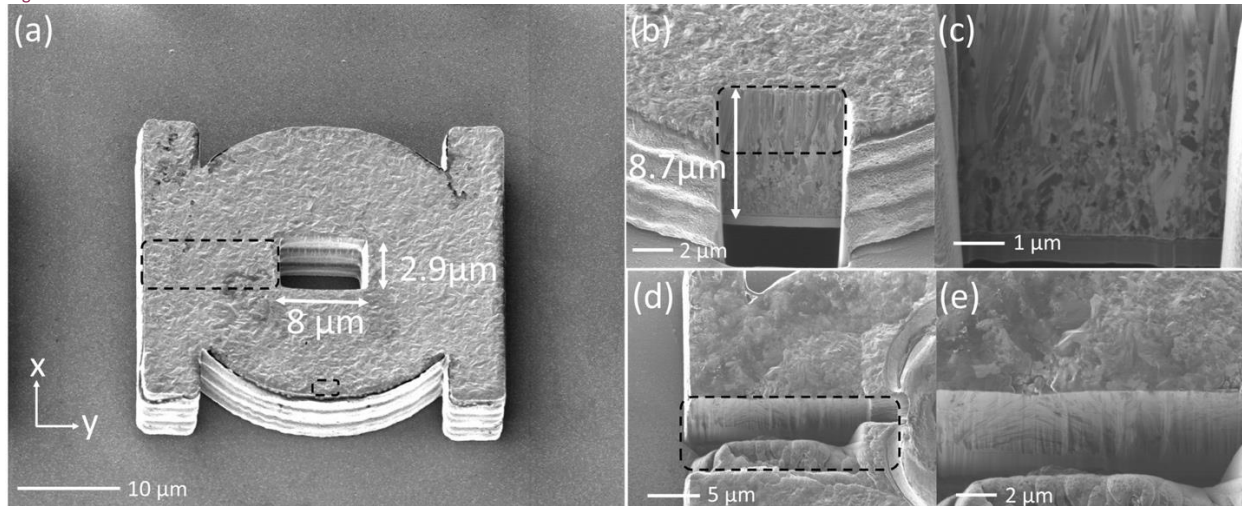


Figure 4. FIB images of Ni CBD specimens, after the electrodeposition and polymer removal. (a) top view; (b) –(e) FIB sections revealing complex Ni microstructures

Fig. 5 shows a different sample with a 9x10 array of fabricated specimens. The 9 rows (from top to bottom) correspond to the nominal slot widths of 2, 3, 4, 2, 3, 4, 2, 3 and 4 μm. The specimens in this case are 13 μm high, much thicker than the ones in Fig. 4. Some of the specimens have moved around, after the polymer was removed, suggesting a low adhesion, which should make their removal for fracture testing easier.

Alternatively, tungsten, W, was also deposited using an AJA Orion sputter system. A 4.7 μm layer of W was DC sputtered (direct current) from a 3 inch target at 150 W using argon plasma. An uniform FIB cross-section of the layer is shown in Fig. 6. In order to reduce stress, the pressure was set to 15 mTorr during deposition. To prevent temperature from rising, the deposition was run in 9 intervals with cooling steps in-between.

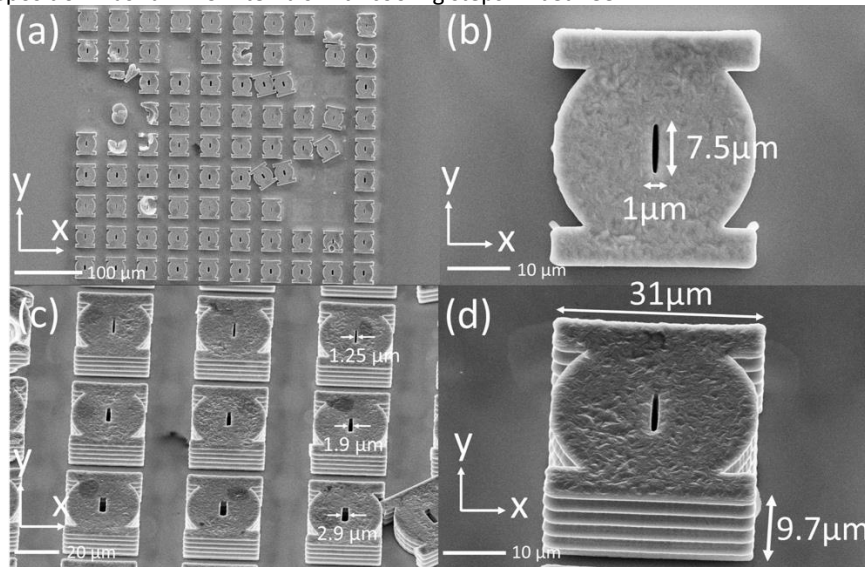


Figure 5. (a) SEM images of an array of CBD specimens. (b) Zoom in of a single CBD. (c) Zoom in of 45° view of (a). (d) Zoom in of 45° view of a single CBD.

CONCLUSIONS

This paper for the first time reports how a micro-scale cracked Brazilian disk (CBD) fracture specimens can be fabricated by 2PP-DLW, followed by electrodeposition. Nickel was used in this feasibility study. SEM and FIB imaging

shows that the additively manufactured CBD specimens have sub- μm microstructure with no obvious defects (see Figs. 4 and 6). The immediate future tasks are to further characterize the quality of the obtained samples via atomic probe tomography and nano-indentation, and measure fracture behavior on as received and neutron irradiated specimens. We are also actively working on fabricating W specimens (see Fig. 6), which may require the use of other backfilling techniques, such as sputtering, and vapor phase deposition such as chemical vapor deposition and atomic layer deposition to perform conformal coating on the high-temperature resistant templates made of silica with the double-inverse laser writing processes.

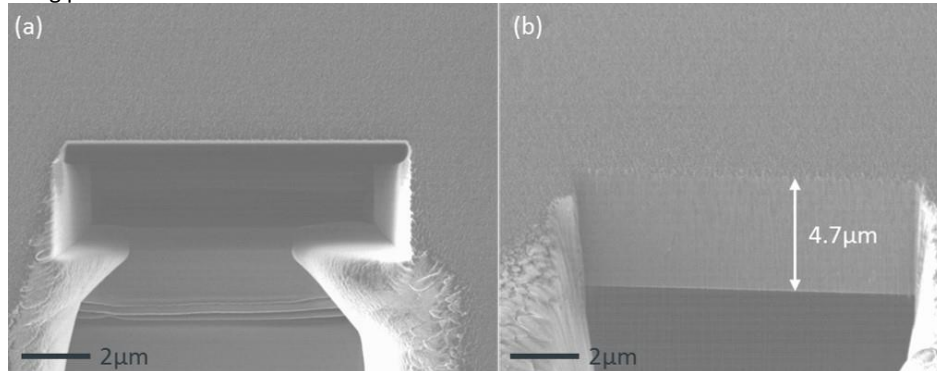


Figure 6. An FIB cross-section of the tungsten (W) deposition on silica substrate using DC sputtering process. (a) Top view and (b) cross-sections are cut using a focus ion beam.

ACKNOWLEDGEMENTS

The authors would like to thank Dr. Sam Ladak (Cardiff University) for the use of the electroplating system for structure fabrication. This work was supported by the EPSRC grant EP/P034446/1 “Structural integrity characterization of nuclear materials via nano additive manufacturing”.

REFERENCES

1. M. Klimenkov, U. Juntsch, M. Rieth, *et al.*, *Nuclear Materials and Energy* 1–4 (2016).
2. S. Nagata, H. Katsui, K. Hoshi, *et al.*, *Journal of Nuclear Materials* 442 328–332 (2013).
3. E. M. Grieveson, D. E. J. Armstrong, S. Xu, and S.G. Roberts, *J. Nucl. Mater.* 430, 119–124(2012).
4. M. Mostafavi, R. Bradley, D. E. J. Armstrong, and T. J. Marrow, *Sci. Rep.* 6 (2016).
5. K. Thompson, B. Gorman, D. Larson, B. van Leer, and L. Hong, *Microsc. & Microanalysis* 12, 1736 (2006).
6. Z. Wang, T. Kato, T. Hirayama, N. Kato, K. Sasaki, and H. Saka, *Appl. Surf. Sci.* 241, 80–86 (2005).
7. B.R. Jany, K. Szajna, M. Nikiel, D. Wrana, E. Trynkiewicz, R. Pedrys, F. Krok. *Appl. Surf. Sci.* 327, 86–92 (2015).
8. J. Mayer, L.A. Giannuzzi, T. Kamino and J. Michael, *MRS Bulletin* 32, 400–407 (2007).
9. Stratulat, D. E. J. Armstrong, S. G. Roberts, *Corrosion Sci.* 104, 9–16(2016).
10. G. von Freymann, A. Ledermann, M. Thiel, I. Staude, S. Essig, K. Busch and M. Wegener, *Adv. Funct. Mater.* 20, 1038 (2010).
11. L.-F. Chen, M. P. C. Taverne, X. Zheng, J.-D. Lin, R. Oulton, M. Lopez-Garcia, Y.-L. D. Ho, J. G. Rarity, *Opt. Express* 23, 26565-26575 (2015)
12. G. I. Williams, M. Hunt, B. Boeheme, M. Traverne, Y.-L. D. Ho, S. Giblin, D. E. Read, J. G. Rarity, R. Allenspach, and S. Ladak, *Nano Res.* (2017). doi:10.1007/s12274-017-1694-0.